
1 **Class II *LBD* genes *ZmLBD5* and *ZmLBD33* regulate gibberellin and**
2 **abscisic acid biosynthesis**

3 Jing Xiong,^{a,2} Xuanjun Feng,^{a,b,2,3} Weixiao Zhang,^a Xianqiu Wang,^a Yue Hu,^a Xuemei
4 Zhang,^a Fengkai Wu,^a Wei Guo,^a Wubing Xie,^a Qingjun Wang,^a Jie Xu,^{a,b} Yanli Lu,^{a,b,4}

5

6 ^aMaize Research Institute of Sichuan Agricultural University, Wenjiang, Sichuan, 611130,
7 China;

8 ^bState Key Laboratory of Crop Gene Exploration and Utilization in Southwest China,
9 Wenjiang, Sichuan, 611130, China;

¹This work was supported by the National Natural Science Foundation of China (Grant: 32030078) and the Foundation of international cooperation in science and technology of Chengdu, China (Grant: 2020-GH02-00027-HZ) (to Y.L.), and the National Natural Science Foundation of China (Grant: 31801371) and the Applied basic research program of Sichuan province, China (Grant: 2020YJ0350) (to X.F.).

10

11 ²These authors contribute equally to this work.

12 ³Senior author

13 ⁴Author for contact: Yanli Lu (yanli.lu82@hotmail.com).

14 The author responsible for distribution of materials integral to the findings presented in this
15 article in accordance with the policy described in the Instructions for Authors
16 (www.plantphysiol.org) is: Yanli Lu (yanli.lu82@hotmail.com).

17

18

19

20

21

22

23

24 **Author Contributions**

25 X.F. and Y.L. designed the research. J.X., W.Z., X.W., Y.H. and X.Z. performed the main
26 part of experiment. X.F., Q.W, W.G., W.X. and F.W. performed the field investigation of
27 plant phenotype. J.X. and Y.L. are responsible for managing materials related to the
28 project. X.F. and J.X. analyzed data and prepared the figures. X.F., J.X. and Y.L. wrote the
29 manuscript.

30

31

32 **Class II *LBD* genes *ZmLBD5* and *ZmLBD33* regulate gibberellin and**
33 **abscisic acid biosynthesis**

34

35 **ABSTRACT**

36 Lateral organ boundaries domain (LBD) proteins are plant-specific
37 transcription factors. Class I *LBD* members are widely reported to be pivotal for
38 organ development, however, the role of class II members is unknown in
39 cereal crops. Class II LBD proteins are distinguished from class I by the lack of
40 a Gly-Ala-Ser (GAS) peptide and leucine-zipper-like coiled-coil domain, which
41 is thought to be essential for protein dimerization. In this study, *ZmLBD5* and
42 *ZmLBD33* form homo- and hetero-dimers, like class I members. At seedling
43 stage, *ZmLBD5* promoted biomass accumulation (shoot dry weight and root
44 dry weight), root development (root length, root number, and root volume), and
45 organ expansion (leaf area), while *ZmLBD33* repressed these processes and
46 display a dwarf phenotype. Both *ZmLBD5* and *ZmLBD33* displayed negative
47 roles in drought tolerance mainly by increasing stomatal density and stomatal
48 aperture. RNA sequencing, gene ontology enrichment analysis, and transient
49 luciferase expression assays indicated that *ZmLBD5* and *ZmLBD33* are mainly
50 involved in the regulation of the *TPS-KS-GA2ox* gene module, which
51 comprises key enzymatic genes upstream of GA and ABA biosynthesis. GA_1
52 content increased in *ZmLBD5*-overexpressing seedlings, while GA_3 and
53 abscisic acid content decreased in both transgenic seedlings. Consequently,
54 exogenous GA_1 or GA_3 undoubtedly rescued the dwarf phenotype of
55 *ZmLBD33*-overexpressing plants, with GA_1 performing better. The study of
56 *ZmLBD5* and *ZmLBD33* sheds light on the function of the class II *LBD* gene
57 family in maize.

58

59

60 **INTRODUCTION**

61 Gibberellins (GAs) and abscisic acid (ABA) are two phytohormones derived
62 from isopentenyl diphosphate (IPP). In plastids, IPP is converted to
63 monoterpenes (C_{10}) and geranylgeranyl diphosphate (C_{20} , GGPP). At GGPP
64 the pathway in plastids branches out in several directions, with separate
65 pathways leading to the *ent*-kaurenoids and GAs (C_{20}), the phytol side-chain of

66 chlorophyll (C₂₀), phytoene and carotenoids (C₄₀), and the nonaprenyl (C₄₅)
67 side-chain of plastoquinone (Hedden and Sponsel, 2015; He et al., 2020).
68 Thus, manipulation of one of the pathways can have significant effects on the
69 flux through other branches, and any regulation in the pathway upstream of
70 GGPP will affect all branches. In GA biosynthesis, GGPP is first cyclized to
71 *ent*-copalyl diphosphate (CPP) by CPP synthases (CPSs) and then converted
72 to *ent*-kaurene by *ent*-kaurene synthases (KSs) (Hedden and Sponsel, 2015;
73 He et al., 2020). This is followed by oxidative reactions catalyzed by
74 cytochrome P450 oxygenases and 2-oxoglutarate-dependent oxygenases that
75 regulate the dynamic balance between activation and deactivation of GAs
76 (Hedden and Proebsting, 1999; Fu et al., 2016).

77 GAs and ABA are two of the most studied phytohormones in plants. The
78 essential role of GAs in shoot elongation has been demonstrated clearly in a
79 large number of studies (Spray et al., 1996; Teng et al., 2013; Chen et al., 2014;
80 Nagai et al., 2020). In addition, GAs regulate various aspects of plants, such
81 as flowering (Bao et al., 2020), root development (Zimmermann et al., 2010),
82 seed development (White et al., 2000), and stress response (Colebrook et al.,
83 2014), and the “green revolution” of farming occurred largely owing to the
84 application of *GA20ox* knockout crops (Hedden, 2003). ABA has multiple
85 functions, and it is well known to ameliorate abiotic stress. Under the stress of
86 drought, ABA accumulates rapidly and plays a positive role in drought
87 tolerance by regulating multiple processes at different tiers, such as the
88 expression of ABA-responsive genes, stomatal closure, root growth, and the
89 production of protective metabolites (Mehrotra et al., 2014). ABA is mainly
90 produced from the cleavage of carotenoids (Sponsel and Hedden, 2010; Xiong
91 and Zhu, 2003), which are co-derived from GGPP along with GAs (Sponsel
92 and Hedden, 2010). Thus, the crosstalk between GAs and ABA biosynthesis is
93 universal.

94 Lateral organ boundaries domain (LBD) proteins are plant-specific
95 transcription factors (Shuai et al., 2002; Majer and Hochholdinger, 2011; Xu et
96 al., 2016). Characteristically, they comprise a cysteine C-block (CX₂CX₆CX₃C)
97 required for DNA-binding activity, a Gly-Ala-Ser (GAS) block, and a leucine
98 zipper-like coiled-coil motif (LX₆LX₃LX₆L) responsible for protein dimerization
99 (Shuai et al., 2002; Majer and Hochholdinger, 2011; Xu et al., 2016). Based on

100 the conserved domains, LBD genes have been identified and classified into
101 two groups (class I and class II) (Shuai et al., 2002; Majer and Hochholdinger,
102 2011; Zhang et al., 2014; Yu et al., 2020). Class I, comprising most of the
103 members, is characterized by a GAS and leucine-zipper-like coiled-coil domain,
104 while class II members have no or an incomplete GAS and leucine zipper-like
105 coiled-coil domain. It is thought that these differences underlie the functional
106 diversity between class I and class II members (Majer and Hochholdinger,
107 2011; Xu et al., 2016). Class I members have been mostly reported to play an
108 important role in auxin response and plant development (Majer and
109 Hochholdinger, 2011), such as maintaining the indeterminate cell state in the
110 shoot apical meristem (SAM) (Semiarti et al., 2001; Iwakawa et al., 2007),
111 female gametophyte development (Evans, 2007), inflorescence architecture
112 (Bortiri et al., 2006), and formation of seminal and shoot-borne root primordia
113 (Taramino et al., 2007; Majer et al., 2012; Xu et al., 2015). In contrast, there
114 are few reports about class II members, and their functions are unclear. The
115 class II *LBD* genes that have been characterized thus far are not involved in
116 development but in metabolism, such as anthocyanin biosynthesis and
117 nitrogen metabolism (Rubin et al., 2009; Albinsky et al., 2010; Majer and
118 Hochholdinger, 2011). Although the phylogenetic characteristics of the *LBD*
119 family in maize have been reported (Zhang et al., 2014), there are no reports
120 about the function of class II *LBDs* in cereal crops.

121 In this study, two class II *LBD* maize genes, *LBD5* and *LBD33*, with high
122 identity (Zhang et al., 2014), were investigated. Here we found homo- and
123 hetero-dimerization in both *LBD5* and *LBD33*. This is at odds with the
124 hypothesis that the GAS and leucine-zipper-like coiled-coil domain is essential
125 for dimerization in *LBDs*. In addition, *LBD5* and *LBD33* play a role in the
126 regulation of the core module in GA biosynthesis and affect the final output of
127 GAs and ABA. This work may contribute to the initial understanding of the
128 biological function of cereal class II *LBD* genes in cereal crops, and provide a
129 new insight into the response of drought in maize.

130
131

132 **RESULTS**

133 **LBD5 and LBD33 can form homodimers and heterodimers**

134 Given that the GAS and leucine-zipper-like coiled-coil domain of class I
135 members is essential for protein dimerization and class II members are
136 characterized by the lack of or an incomplete domain, the ability of LBD5 and
137 LBD33 to dimerize was tested. Although LBD5 and LBD33 have no GAS and
138 leucine-zipper-like coiled-coil domain, homo- and hetero-dimerization were
139 clearly detected through Y2H and BiFC assays (Fig. 1, A and B). Additionally,
140 LBD5 and LBD33 displayed weak interactions with the class I member LBD44
141 (Fig. 1, A and B). To identify the critical domain for dimerization, LBD5 and
142 LBD33 were cleaved optionally at two sites, and six kinds of peptides were
143 obtained for Y2H assays (Supplemental Fig. S1A). Parts A, B, and C represent
144 the N terminal C-block (CX2CX6CX3C), the GAS and leucine-zipper-like
145 coiled-coil (LX6LX3LX6L) domain, and the C terminal domain, respectively
146 (Fig. S1A). Unfortunately, we failed to clearly identify which part is responsible
147 for protein-protein interaction (Supplemental Fig. S1B), but we proposed that
148 the C part may have a positive effect on dimerization both in LBD5 and LBD33
149 (Supplemental Fig. S1B).

150 **Effects of LBD5 and LBD33 on organ development and drought tolerance**

151 To investigate the role of *LBD5* and *LBD33* in plant development or
152 environmental stimuli, first their tissue-specific expression and stimuli
153 responses were profiled. *LBD5* and *LBD33* were widely expressed in various
154 tissues and relatively higher in roots (Supplemental Fig. S2A). Therefore, the
155 response of *LBD5* and *LBD33* to eight phytohormones related to stress
156 response and organ development was investigated in the roots of seedlings.
157 *LBD5* and *LBD33* were induced most strongly by GA₃ and JA, and these
158 stimuli had similar effects (Supplemental Fig. S2B). In addition, responses to
159 PEG, nitrogen deficiency, and phosphorus deficiency were investigated in the
160 root and leaf. *LBD5* and *LBD33* were remarkably induced by PEG-mimic
161 drought stress and nitrogen deficiency in the root. However, responses in the
162 leaf were weak and differed slightly between *LBD5* and *LBD33* (Supplemental
163 Fig. S1, C and D).

164 *LBD5* and *LBD33* were overexpressed, which were called LBD5(OE) and
165 LBD33(OE) hereafter, in a wild-type maize line KN5585. More than seven

166 transgenic lines of each gene were constructed and transcript levels of *LBD5*
167 and *LBD33* were measured. Three representative transgenic lines of each
168 gene were used for further study after the detection of expression levels
169 (Supplemental Fig. S3A). Homozygous lines were hybridized with the wild type,
170 and the hybrid F1 progenies were used for phenotype investigation. During
171 germination and the early seedling stage there was no difference between
172 *LBD5*(OE), *LBD33*(OE), and the wild type (Supplemental Fig. S3B). About 6
173 days after germination, an obvious dwarf phenotype of *LBD33*(OE) was
174 observed. About 12 days after germination, *LBD5*(OE) was noticeably taller
175 than the wild type. Detailed analysis showed that the shoot length, leaf area,
176 and biomass were remarkably affected by the over expression of *LBD5* and
177 *LBD33*, and all of these phenotypic values increased in *LBD5*(OE) but
178 decreased in *LBD33*(OE) (Fig. 3 and Supplemental Fig. S3D). To investigate
179 the change at the micro-level, leaf cell length and width was observed. As
180 expected, cells were longer in *LBD5*(OE) and shorter in *LBD33*(OE) than that
181 in the wild type (Supplemental Fig. S4). Unexpectedly, *LBD33*(OE) plants
182 possessed narrower leaves but wider cells and *LBD5*(OE) possessed wider
183 leaves but narrower cells than the wild type (Supplemental Fig. S4). We thus
184 speculated that the leaf cell number may be lower in *LBD33*(OE) and higher in
185 *LBD5*(OE). To investigate the effects on below-ground parts, seedlings were
186 grown in hydroponic conditions. The root number, primary root length, root
187 surface area, root volume, shoot fresh weight, and root fresh weight were all
188 greater in *LBD5*(OE) and lesser in *LBD33*(OE) than that in the wild type
189 (Supplemental Fig. S3, C and D). However, the difference in root dry weight
190 between *LBD5*(OE), *LBD33*(OE), and the wild type was not significant when
191 grown in soil (Fig. 2B).

192 Given the strong response of *LBD5* and *LBD33* to PEG-mimic drought
193 stress, wild type and different transgenic lines were grown in separate pots
194 and exposed to water deficiency. Both *LBD5*(OE) and *LBD33*(OE) displayed
195 earlier withering than the wild type, and this effect was more remarkable in
196 *LBD5*(OE) than in *LBD33*(OE) (Fig. 2A). The biomass penalty under water
197 deficient conditions also indicated that *LBD5*(OE) and *LBD33*(OE) were more
198 sensitive to drought stress than the wild type when grown in separate pots (Fig.
199 2, B-D).

200 However, after anthesis in the field, the ear height and the internode length
201 of lines 5-2 and 5-4 were shorter than that of the wild type (Supplemental Fig.
202 S5C and Table S1). However, the effect of LBD5 on plant height was not clear,
203 because line 5-1 was taller, line 5-2 was shorter, and line 5-4 was similar when
204 compared with the wild type (Supplemental Fig. S5, A and B). The increase in
205 plant height of line 5-1 may be attribute to the larger number of internodes
206 (Supplemental Fig. S5D). Thus, we speculate that LBD5 may have a positive
207 effect on internode number and a negative effect on internode length.
208 LBD33(OE) plants were significantly shorter than the wild type owing to the
209 decrease in internode length but not internode number (Supplemental Fig. S5,
210 A-D and Table S1). Grain yields upon well-watering and drought stress
211 conditions supported the drought sensitive phenotype of LBD5(OE) and
212 LBD33(OE) (Fig. 2, G-I). In addition, *LBD5* and *LBD33* negatively regulate
213 grain yield with different mechanism. *LBD33* decreased ear size and
214 hundred-grain weight simultaneously, while *LBD5* mainly decreased ear size
215 (Fig. 2, G-I and Supplemental Fig. S5, E and F).

216 **LBD5 and LBD33 promote water loss by increasing stomatal density and** 217 **stomatal aperture**

218 To unravel the underlying mechanism by which LBD5(OE) and LBD33(OE)
219 increased sensitivity to drought stress, the rates of water loss (RWL) of
220 detached leaves were measured. LBD5(OE) and LBD33(OE) had significantly
221 higher RWL than the wild type (Fig. 3A). The stronger water loss in LBD5(OE)
222 and LBD33(OE) may have, consequently, resulted in earlier soil drought after
223 the outage of water. Thus, the soil moisture content (SMC) was analyzed.
224 Fifteen days after the outage of water SMC was lowest in LBD5(OE) and
225 remarkably lower in LBD33 (OE) than in the wild type (Fig. 3B). Further, the
226 stomatal density and open-closed-ratio (OCR) were investigated. To measure
227 OCR, leaves were detached from 12-day-old seedlings and dehydrated for 12
228 minutes in original growing conditions. Interestingly, LBD5(OE) and LBD33(OE)
229 had higher stomatal density and OCR than the wild type (Fig. 3, C and D and
230 Supplemental Fig. S6A).

231 In addition, stomatal aperture after ABA or H₂O₂ stimulation was investigated.
232 Detached leaves were pretreated with stomatal opening buffer to get the
233 maximum degree of stomatal openness. Then, ABA or H₂O₂ was added, and

234 stomatal aperture was fixed at different times. The stomatal aperture of
235 LBD5(OE) and LBD33(OE) was greater than that of wild type, upon both ABA
236 and H₂O₂ treatment (Supplemental Fig. S6, B and C). ABA and H₂O₂ are both
237 powerful stimulators of stomatal closure. These results indicated that
238 overexpression of *LBD5* or *LBD33* could reduce the sensitivity of stomata to
239 ABA and H₂O₂.

240 To determine if there were other factors that made LBD5(OE) and
241 LBD33(OE) more sensitive to drought stress, transgenic and wild-type plants
242 were grown in the same pots to test the difference in drought tolerance.
243 LBD5(OE), LBD33(OE), and the wild type withered at almost the same time
244 after the outage of water. However, the penalty of shoot dry weight upon
245 drought stress was greater in LBD5(OE) and LBD33(OE) (Fig. 3E). These
246 results suggest that enhanced water loss from stomata was one cause of
247 drought sensitivity in LBD5(OE) and LBD33(OE) plants.

248 **LBD5 and LBD33 may function in the GGPP–CPP–kaurene/acid–GA** 249 **metabolic pathway**

250 As transcription factors, overexpression of LBD5 or LBD33 may widely affect
251 the expression of downstream target genes, leading to the final phenotype.
252 Therefore, RNA-seq was performed using 12-day-old seedlings to profile the
253 change of gene expression in LBD5(OE) and LBD33(OE) compared with the
254 wild type. A total of 1844 and 1174 differentially expressed genes (DEGs)
255 were identified in LBD5 (OE) and LBD33(OE), respectively (Fig. 4A and
256 Supplemental Table S2). There were 666 members in the intersection of DEGs
257 between LBD5(OE) and LBD33(OE), and almost all of these genes displayed
258 a similar expression change in LBD5(OE) and LBD33(OE) when compared to
259 the wild type (Fig. 4A). Of the 666 shared DEGs, 417 were down regulated (Fig.
260 4A). When DEGs from LBD5(OE) and LBD33(OE) were combined, the 3018
261 total genes could be clustered into 6 groups based on the change in
262 expression level (Fig. 4B). Almost all of the shared 666 genes were found in
263 group 2 or group 5, in which genes displayed a similar expression change in
264 LBD5(OE) and LBD33(OE) compared to the wild type. It is plausible that the
265 similar phenotype of LBD5(OE) and LBD33(OE) is caused by the 666 shared
266 DEGs or the other members of group 2 and group 5.

267 Further, DEGs of LBD5(OE) and LBD33(OE) were used for Gene Ontology
268 (GO) enrichment analysis. Results provided a similar and reliable biologic
269 process for LBD5(OE) and LBD33(OE), namely terpenoid biosynthesis (Fig.
270 4C and Supplemental Table S3). A total of 15 DEGs annotated in terpenoid
271 biosynthesis were mainly involved in the GGPP–CPP–kaurene/acid–GA
272 pathway (Fig. 5A). Five of the six genes involved in GGPP biosynthesis were
273 down-regulated in LBD5(OE) and LBD33(OE) (Fig. 5A). We speculated that
274 those 15 genes may be downstream targets of LBD5 and LBD33.

275 **LBD5 and LBD33 directly regulate the *TPS-KS-GA2ox* gene module**

276 To investigate whether LBD5 and LBD33 directly regulate the transcription of
277 candidate target genes, promoters of the candidate genes were cloned for
278 yeast one-hybrid assays. Firstly, the full length of LBD5 and LBD33 were used
279 for the Y1H assays along with 5 candidate promoters. However, none of the
280 five promoter-driven *LacZ* reporter genes could be activated by LBD5 or
281 LBD33 (Supplemental Fig. S7A). Given that most genes were down-regulated
282 by LBD5 and LBD33, we speculated that full length LBD5 and LBD33 may
283 have transcriptional inhibitory activity and block the activation of reporter gene.
284 Therefore, LBD5 and LBD33 were cleaved optionally at two sites and six kinds
285 of peptides were obtained, as shown in Figure S1A, to test the transcriptional
286 inhibitory activity. Full length LBD5, LBD5-BC, LBD33-B, and LBD33-BC
287 displayed remarkable transcriptional inhibitory activity (Supplemental Fig. S7B).
288 LBD5-AB and LBD33-AB, which contained the C-block for DNA binding, had
289 no transcriptional inhibitory activity. Therefore, LBD5-AB and LBD33-AB were
290 then used for Y1H assays along with 15 promoters. LBD5-AB and LBD33-AB
291 could bind to 9 and 5 promoters, respectively (Fig. 5B).

292 Given that LBD proteins are plant specific transcription factors, the
293 regulation of 15 candidate target genes by LBD5 and LBD33 was investigated
294 in plant cells. The promoters of candidate genes were cloned to drive the
295 expression of the *LUC* reporter gene. CaMV35S-controlled *LBD5* or *LBD33*
296 was fused with *GFP* and transiently co-expressed with each
297 candidate-promoter-driven *LUC* in tobacco. Compared with the fold-change of
298 transcription level, luciferase enzymatic activity assays showed that 13 and 11
299 candidate promoters displayed similar behavior upon the overexpression of
300 *LBD5* and *LBD33*, respectively (Fig. 5, A and B). Taking Y1H and

301 dual-luciferase expression assays into consideration, we identified that LBD5
302 and LBD33 directly regulated 7 and 5 of the 15 candidate target genes,
303 respectively.

304 **LBD5 and LBD33 affect seedling size by modulating GA biosynthesis**

305 In plants, ABA is mainly produced from the cleavage of carotenoids (Sponsel
306 and Hedden, 2010; Xiong, 2003), which are co-derived from GGPP along with
307 GAs. Aforementioned results indicated that LBD5 and LBD33 negatively
308 regulate drought tolerance by inhibiting stomatal closure, a process in which
309 ABA is important. Therefore, concentrations of ABA and GAs (the main
310 bioactive form GA₁, GA₃, GA₄, and GA₇) (Hedden and Phillips, 2000), two
311 kinds of phytohormone downstream of GGPP, were measured using
312 12-day-old seedlings. ABA and GA₃ contents were lower in both LBD5(OE)
313 and LBD33(OE) than in the wild type (Fig. 6A). Interestingly, GA₁ content was
314 higher in LBD5(OE) than in the wild type (Fig. 6A). This may explain why
315 LBD5(OE) seedlings were taller than the wild type. However, it is difficult to
316 determine the causal gene from the 15 candidate genes based on the subtly
317 different responses to LBD5 and LBD33 overexpression. Most redox reactions
318 in GA metabolism are catalyzed by cytochrome P450s (He et al., 2020;
319 Hedden and Sponsel, 2015; Sponsel and Hedden, 2010), and 44 cytochrome
320 P450 members were identified in the top enriched GO term (Supplemental
321 Table S3). Thus, the expression change of these 44 members may also
322 contribute to the change in GAs and ABA in LBD5(OE) and LBD33(OE).

323 GAs widely affect plant development, particularly stem elongation (Spray et
324 al., 1996; Teng et al., 2013; Chen et al., 2014; Nagai et al., 2020). To test the
325 causality of GA₁ and GA₃ content on the dwarf phenotype of LBD33(OE)
326 seedlings, exogenous GA₁ and GA₃ were applied in hydroponic conditions.
327 The application of GA₁ and GA₃ remarkably promoted the growth of
328 LBD33(OE) seedlings and reduced the difference between LBD33(OE) and
329 the wild type (Fig. 6A). GA₁ displayed a well phenotypic compensatory effect at
330 0.05 µg/mL (Fig. 6, B and C). However, the effect of GA₃ was weak at 0.05
331 µg/mL, and a higher concentration was needed to better rescue the dwarf
332 phenotype of LBD33(OE) seedlings (Fig. 6, B and C). Therefore, GA₁ may
333 exhibit the dominant effect on shoot growth and elongation at the seedling
334 stage in maize.

336 **DISCUSSION**

337 Class I members of the LBD gene family are involved in the regulation of
338 almost all aspects of plant development, including embryo, root, leaf, and
339 inflorescence development (Majer and Hochholdinger, 2011). However, there
340 are few reports to date on the function of class II members. Characterized
341 class II members, *AtLBD37*, *AtLBD38*, and *AtLBD39*, are not involved in
342 development but in anthocyanin biosynthesis and nitrogen metabolism
343 (Scheible et al., 2004; Rubin et al., 2009; Albinsky et al., 2010; Majer and
344 Hochholdinger, 2011). Here, we investigated the function of two members of
345 the class II *LBD* genes in maize. Multiple lines of evidence suggested that
346 *ZmLBD5* and *ZmLBD33* are involved in the regulation of terpenoid metabolism,
347 and consequently determine GA and ABA content, thus affecting plant
348 development and drought response.

349 Class I members of the LBD protein family are distinguished from class II
350 members by the existence of the GAS and leucine-zipper-like coiled-coil
351 domain (Majer and Hochholdinger, 2011; Xu et al., 2016). This domain is
352 thought to be required for protein dimerization (Majer and Hochholdinger, 2011;
353 Xu et al., 2016). In this study, LBD5 and LBD33, which are class II members
354 lacking a typical GAS and leucine-zipper-like coiled-coil domain, formed
355 homodimers and heterodimers like class I members, implying the typical GAS
356 and leucine-zipper-like coiled-coil domain is not essential for dimerization.
357 However, no domain responsible for dimerization has been identified in LBD5
358 and LBD33. Heterodimerization between LBD5 and LBD33 was strong.
359 However, the interaction was weak when LBD44, a class I member, was used
360 to form heterodimers with LBD5 or LBD33. These results imply that similarity
361 between sequences may facilitate dimerization between LBD monomers.

362 DEGs in *LBD5*- and *LBD33*-overexpressing plants compared to the wild type
363 are perfectly enriched in the same biological process upstream of GA
364 biosynthesis, which was reminiscent of the similar and drastic responses of
365 *LBD5* and *LBD33* to GA₃ treatment. GA₃ content decreased in both LBD5(OE)
366 and LBD33(OE), which is consistent with the down-regulation of most DEGs in
367 the GGPP–CPP–kaurene/acid–GA metabolic pathway. In line with the
368 down-regulation of most DEGs, LBD5 and LBD33 have transcriptional
369 inhibitory activity. Application of exogenous GA₁ and GA₃ clearly restored the

370 dwarf phenotype of LBD33(OE), particularly for shoot length and shoot fresh
371 weight, indicating that decreased GA₁ and GA₃ content are the immediate
372 cause of the dwarf phenotype. Although the expression change of most
373 enriched genes was similar, GA₁ increased in LBD5(OE) and remained
374 unchanged in LBD33(OE), which may explain the taller phenotype of
375 LBD5(OE). GA₁ has been identified in 86 plants, more than any other GA, and
376 studies utilizing single gene dwarf mutants have shown that it is the major
377 bioactive form involved in stem elongation in *Zea mays* and *Pisum sativum*
378 (Sponsel and Hedden, 2010; Spray et al., 1996). Our results also attest that
379 GA₁ has a higher bioactivity, because low concentrations of GA₁ rescued the
380 dwarf phenotype of LBD33(OE) as well as high concentrations of GA₃.

381 ABA is the most important signal in drought response. Under water deficient
382 conditions, ABA accumulates rapidly and leads to stomatal closure to limit
383 transpirational water loss (Mehrotra et al., 2014). In *LBD5*- and *LBD33*-
384 overexpressing plants, the ABA content was decreased probably due to the
385 down-regulation of genes involved in the biosynthesis of the upstream GGPP.
386 As a result, LBD5(OE) and LBD33(OE) had larger stomatal apertures and
387 enhanced transpirational water loss compared with the wild type. However, the
388 mechanism by which *LBD5* and *LBD33* reduce the sensitivity of stomata to
389 exogenous ABA and H₂O₂ is not clear.

390 In addition, *LBD5* and *LBD33* increased stomatal density. Although there are
391 few reports on the involvement of *LBD* genes in the regulation of stomatal
392 density, *GID1*, a very important receptor of GA, plays a negative role in
393 stomatal density in rice (Du et al., 2015). The *gid1* mutant displays extreme
394 dwarfism, increased stomatal density and decreased stomatal sensitivity to
395 water deficiency (Du et al., 2015). Here, the phenotypes of LBD5(OE) and
396 LBD33(OE) were similar to that of *gid1*. Further studies are needed to
397 determine if the decrease of GA₃ in LBD5(OE) and LBD33(OE) plants mimics
398 *gid1* or if there exists underlying causality.

399 In conclusion, *ZmLBD5* and *ZmLBD33* are mainly involved in the regulation
400 of the *TPS-KS-GA2ox* gene module, which comprises key enzymatic genes
401 upstream of GA and ABA biosynthesis. Subtle differences in the regulation of
402 these genes led to GA₁ accumulation and a taller phenotype in LBD5(OE)
403 seedlings. Overexpression of *LBD5* and *LBD33* inhibited GA₃ and ABA

404 biosynthesis and resulted in a dwarf phenotype in LBD33(OE) and drought
405 sensitive phenotype in both LBD5(OE) and LBD33(OE). The study of *ZmLBD5*
406 and *ZmLBD33* sheds light on the function of the class II *LBD* gene family in
407 maize.

408 MATERIALS AND METHODS

409 Plant growth and phenotyping

410 To analyze the expression patterns of LBD5 and LBD33 in different maize
411 tissues, the primary roots and coleoptiles were collected from seedlings
412 germinated for 3 days (VE stage); seminal roots and leaves were collected at
413 the three-leaf stage (V1 stage); and aerial root, stem, ear leaf, husk, silk,
414 immature ears, and tassels were collected from the V13 stage in a maize
415 inbred line (B73) for RNA isolation.

416 For stress and phytohormone treatment, two-leaf-stage seedlings were
417 transferred to Hoagland nutrient solution in a greenhouse with a 14-h light/10-h
418 dark photoperiod at 28°C and grown to the three-leaf-stage. Then, seedlings
419 were subjected to polyethylene glycol 6000 (PEG6000) (20% w/v), nitrogen
420 deficiency (0.1 mM nitrogen), phosphorus deficiency (without phosphorus),
421 ABA (10 µM), GA₃ (1 µM), ethephon (50 µM), indoleacetic acid (IAA) (5 nM),
422 jasmonic acid (JA) (20 µM), salicylic acid (SA) (2 mM), 6-benzyl aminopurine
423 (6-BA) (4 µM), or brassinolide (100 nM). For PEG, nitrogen deficiency, and
424 phosphorus deficiency, root and leaf tissues were harvested after 0, 1, 3, 6, 12,
425 24, and 48 hours of treatment. For phytohormone treatment, the roots were
426 collected after 0, 1, 3, 6, 12, and 24 hours of treatment. The harvested
427 samples were frozen immediately in liquid nitrogen and used for RNA isolation.

428 To analyze the root traits, seedlings were grown in rolled-up germination test
429 paper in nutrient solution. After 15 days, root volume and root surface area
430 were analyzed with WinRhizo Pro 2008a, an image analysis system (Regent
431 Instr. Inc., Quebec, 13 Canada) with a professional scanner (Epson XL 1000;
432 Japan). Root number, primary root length, root fresh weight, shoot fresh weight
433 and shoot length (the length of the aerial part when the seedling was fully
434 stretched) were measured manually. To analyze the effect of GA₁ and GA₃ on

435 *ZmLBD33*-overexpressing plants, wild type (KN5585) and overexpression line
436 33-4 were germinated and grown in rolled-up germination test paper in nutrient
437 solution containing GA₁ or GA₃ (0, 0.05, 0.1, 0.5, or 1.0 ng/mL). After 15 days,
438 the shoot length, second leaf area (length × width × 0.75), root fresh weight,
439 and shoot fresh weight were measured manually. Root traits were analyzed
440 with WinRhizo Pro. For each treatment, at least 15 seedlings were used, and
441 each treatment was repeated thrice.

442 For drought stress tests in individual pots, equal volumes of well-mixed soil,
443 containing 200 mL of water, was put in each pot (length × width × height = 10 ×
444 10 × 13 cm), and 5 seedlings of each line were grown in different pots. The
445 control group was well watered, whereas the test group was not watered until it
446 exhibited wilting. The shoot dry weight and root dry weight were measured. To
447 analyze the soil moisture, 1 cm³ soil was sampled from each pot at three
448 different stages (0, 10, and 15 days after planting).

449 For same-pot drought stress tests, larger pots (length × width × height = 54 ×
450 28 × 4 cm) were used. Various transgenic plant lines and wild type plants were
451 grown in the same pot. When test seedlings displayed significant wilting,
452 photographs were taken and shoot dry weight was measured.

453 **Overexpression of *LBD5* and *LBD33***

454 The coding sequence of *ZmLBD5* or *ZmLBD33* was cloned into
455 pCAMBIA3301 between BamH I and Sac I restriction sites and fused with HA
456 and FLAG tags at N- and C- terminals, respectively, and expression was driven
457 by the maize ubiquitin promoter. The vector was introduced into agrobacterium
458 EHA105. Agrobacterium-mediated maize transformation was performed at
459 Weimi Biotechnology (Jiangsu) Co. LTD, and the maize inbred line KN5585
460 was used as a recipient. Basta herbicide (0.3%, [v/v]) and PCR were used to
461 identify transgenic plants.

462 **Yeast two-hybrid (Y2H) and bimolecular fluorescence complementation** 463 **(BiFC)**

464 To test whether *ZmLBD5* and *ZmLBD33* forms dimer with other LBDs or

465 itself, the full codon regions of *ZmLBD5*, *ZmLBD33*, and *ZmLBD44* were
466 individually cloned into pGBK-T7 and/or pGAD-T7 vector and fused with BD
467 and/or AD. BD-fused *ZmLBD5*, *ZmLBD33*, or *ZmLBD44* was individually
468 co-transformed with AD-fused *ZmLBD5*, *ZmLBD33*, and empty pGAD-T7 into
469 the Y2HGold yeast strain. Yeast cells harboring pGBK-T7 and pGAD-T7
470 vectors were diluted to three concentrations and grown on nonselective
471 (SD/-Trp/-Leu) or selective (SD/-Trp/-Leu/-His/-Ade) medium. A pGBKT7-53
472 and pGADT7-T combination was used as a positive control (+). A
473 pGBKT7-Lam and pGADT7-T combination was used as a negative control (-).
474 To test the effect of different regions, *ZmLBD5* and *ZmLBD33* were segmented
475 into three parts (A: N-terminal C-block domain, B: GAS and leucine-zipper-like
476 coiled-coil domain, and C: C-terminal domain) based on the genome wide
477 analysis of LBD genes in maize (Zhang et al., 2014). For BiFC assays, the full
478 codon regions of *ZmLBD5*, *ZmLBD33*, and *ZmLBD44* were individually cloned
479 into pXYc104 and pXYn106 vectors and fused with the C-terminal (YC) and
480 N-terminal (YN) of YFP. Then, indicated plastid combinations were
481 co-transformed into agrobacterium cells. Transient expression was performed
482 on *N. benthamiana* leaves. Primers and constructions are listed in
483 Supplemental Table S4.

484 **Yeast one-hybrid (Y1H)**

485 To investigate the binding of *ZmLBD5* and *ZmLBD33* to the promoters of
486 candidate genes, *ZmLBD5*, *ZmLBD5AB*, *ZmLBD33*, and *ZmLBD33AB* were
487 inserted into the pJG4-5 vector and fused with a TF-activating domain. The
488 promoters (about 2,000-bp) of 15 candidate genes were inserted into pLacZi2u
489 upstream of the lacZ reporter. Then, these vectors were co-transformed into
490 the yeast strain EGY48, screened upon SD Base (without Trp and Ura, with
491 glucose as the carbon source), and validated by PCR. The positive clones
492 were then transferred to another SD Base [without Trp and Ura, replacing
493 glucose with galactose and raffinose, and containing X-gal
494 (5-bromo-4-chloro-3-indolyl- β -D-galactopyranoside)] for blue color
495 development (Feng et al., 2016).

496 To investigate whether *ZmLBD5* and *ZmLBD33* have transcriptional

497 inhibition activity, A, B, C, AB, BC, and full codon regions of *ZmLBD5* and
498 *ZmLBD33* were amplified and fused with the *Gal4-AD* sequence. Then, the
499 fused fragments were cloned into pGBKT7 and fused with the *Gal4-BD*
500 sequence. *Gal4-AD* was cloned into pGBKT7 and fused with the *Gal4-BD*
501 sequence, and complete *Gal4* was attained and used as a control. The
502 transformation was conducted according to the manual of Yeast Protocols
503 Handbook (Clontech). Primers and constructions are listed in Supplementary
504 Table S4.

505 **Transient dual-luciferase expression assays**

506 Reporters were constructed based on the pGreenII 0800-LUC vector and
507 the effectors were constructed based on the pCAMBIA2300-eGFP vector.
508 About 2,000-bp promoter fragments of candidate genes were amplified from
509 B73 genomic DNA by PCR and cloned into pGreenII-LUC to drive the LUC
510 reporter. *ZmLBD5* and *ZmLBD33* were cloned into pCAMBIA2300-eGFP and
511 driven by the CaMV35S promoter. The empty vector pCAMBIA2300-eGFP
512 was used as a control. Primers and constructions are listed in Supplementary
513 Table S4.

514 Transient dual-luciferase assays were performed in tobacco leaves. A
515 dual-luciferase assay kit (Vazyme, DL101-01) was used for enzymatic activity
516 measurement. Three independent measurements were carried out for each
517 analysis, and four biological repeats were performed.

518 **Measurement of stomatal density and stomatal aperture**

519 At the three-leaf stage, the middle parts of the last fully expanded leaves
520 were used for stomata measurement. The number of stomata in each
521 microscopic field on abaxial leaf and adaxial leaf were calculated using an
522 Olympus microscope (IX73, Japan) with a 10× objective lens. For each line,
523 ten plants were selected for the counting and three replicates were performed.
524 To investigate the ratio of open and closed stomata after dehydration, abaxial
525 leaves were covered with clear nail polish 12 minutes after detachment. The
526 shape of the stomata is stamped into the nail polish film during the rapid curing.
527 The nail polish film was then stripped off and placed on a glass slide for

528 microscopic observation with a 100× objective lens. For the assessment of
529 stomatal closure dynamics induced by ABA and H₂O₂, the detached leaves
530 were floated on stomatal opening buffer (10 mM Tris-HCl, pH 5.6, 10 mM KCl,
531 and 50 μM CaCl₂) for 3 h under light to induce the stomata to open to the
532 maximum extent. Then, 10 μM ABA or 1 mM H₂O₂ was added to induce
533 stomata closure and stomatal aperture was fixed at different time points using
534 nail polish. Stomatal images were analyzed with ImageJ software to measure
535 the aperture size. More than 30 stomata per sample were measured and each
536 treatment included three replicates.

537 **RNA sequencing**

538 RNA sequencing (RNA-seq) was performed on the transgenic lines 5-1,
539 33-5, and the wild type plants. Twelve-day-old seedlings were harvested for
540 total RNA extraction. Sequencing and analysis were entrusted to Beijing
541 Novogene company (<https://www.novogene.com/>) using the Illumina HiSeq
542 4000 sequencing platform.

543 **GA and ABA content**

544 Endogenous GAs (GA₁, GA₃, GA₄, and GA₇) and ABA contents were
545 measured in the overexpression lines 5-1 and 33-4, and in wild-type plants.
546 Approximately 5 g of aerial tissue was harvested from 12-day-old seedlings
547 grown under normal conditions (14-h light/10-h dark photoperiod at 28°C).
548 Measurement of the GA and ABA content was entrusted to Convinced-Test
549 (Nanjing) and analyzed by liquid chromatography-mass spectrometry (LC-MS).
550 Two biological repeats were prepared, and three technical repetitions were
551 performed for each sample.

552 **Real-time quantitative PCR**

553 Total RNA was isolated with a Plant Total RNA Isolation kit (FOREGENE,
554 RE-05014). Genomic DNA in samples was removed with RNase-free DNase I
555 (Trans, GD201-01). RNA concentration was measured by spectrophotometer
556 (NanoDrop 2000C). First-strand cDNA was synthesized using Prime Script RT
557 reagent kit with gDNA Eraser (Takara, RR047A) from DNase I-treated RNA.

558 Real-time quantitative PCR was performed using SYBR Green Fast qPCR Mix
559 (ABclonal, RM21203) and a BioRad CFX96 machine. *ZmeF1a* was used as
560 reference gene to normalize the expression of candidate genes. Primers are
561 listed in Supplemental Table S5.

562 **Statistical Analysis**

563 Unless noted otherwise, data are presented as the mean \pm sd. Statistical
564 significance was determined through one-way ANOVA analysis using
565 GraphPad Prism (version 9.0). Variations were considered significant if P
566 < 0.05 (*), 0.01 (**) or 0.001 (***).

567 **ACCESSION NUMBERS**

568 Sequence data for genes and proteins presented in this article can be found
569 in the *EnsemblPlants* database under the following accession numbers:
570 *ZmLBD5* (Zm00001d029506), *ZmLBD33* (Zm00001d038717), *ZmLBD44*
571 (Zm00001d023316), *ZmEF1a* (Zm00001d046449). The RNA-seq data was
572 deposited in NCBI with BioProject ID: PRJNA715318.

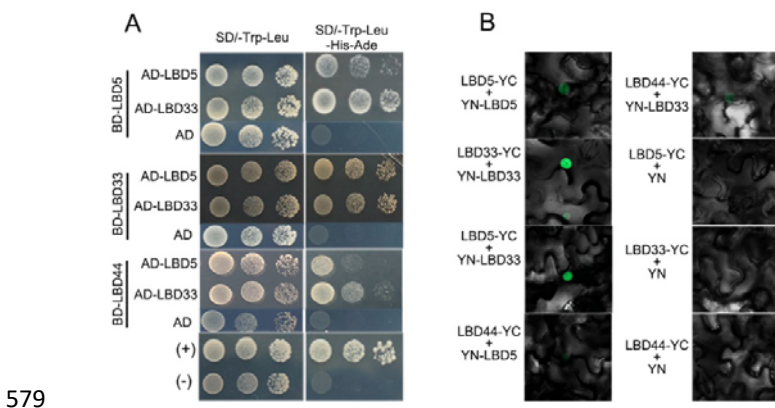
573

574 **ACKNOWLEDGMENTS**

575 We thank Dr. Peter Hedden from Rothamsted Research, UK for his inspiring
576 work and the valuable suggestions on our research.

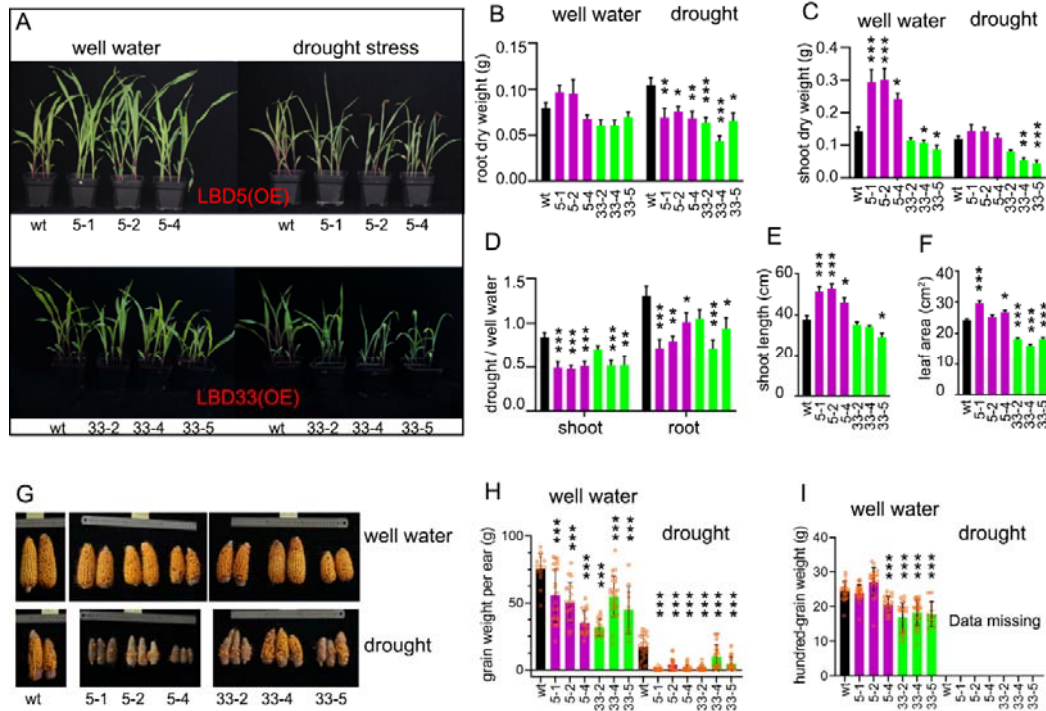
577

578 **Figure Legends**

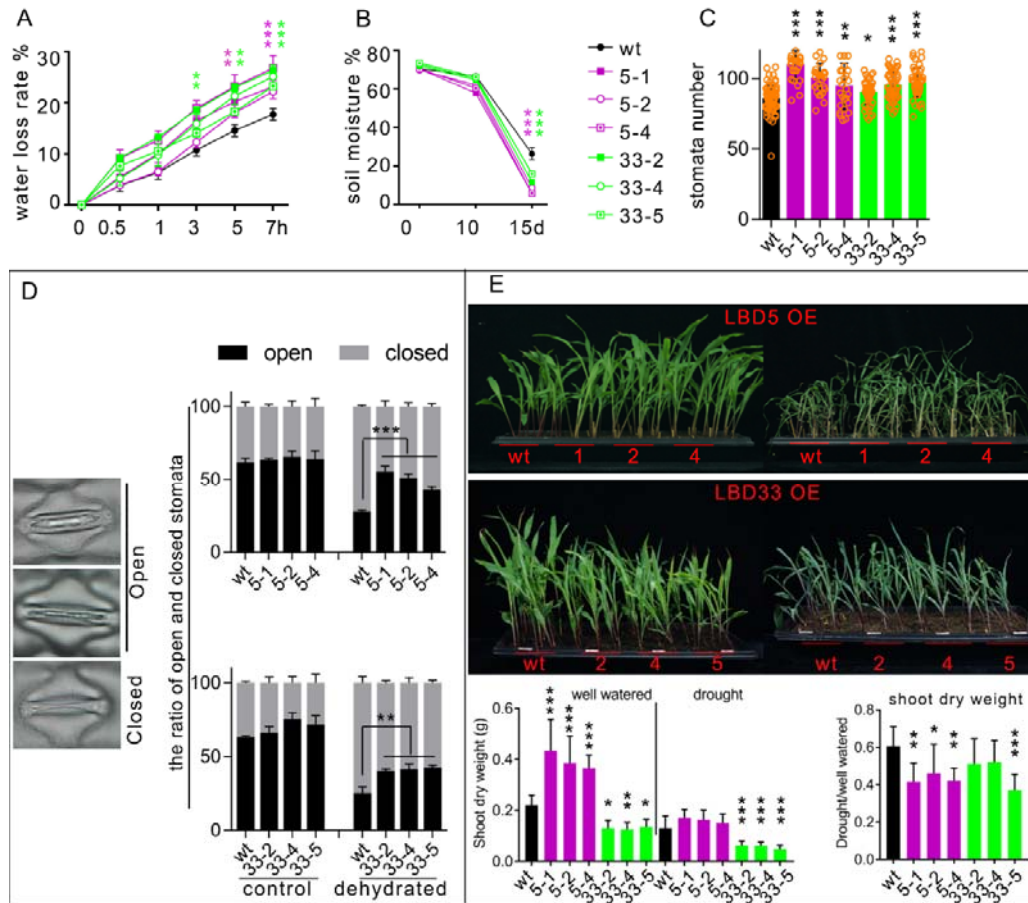


580 **Figure 1. Protein-protein interaction analyzed by yeast two-hybrid and bimolecular**
581 **fluorescence complementation.** Full codon region of *ZmLBD5*, *ZmLBD33*, and
582 *ZmLBD44* were used here. (A) The yeast cells harboring the indicated plasmid
583 combinations were grown on nonselective (SD/-Trp/-Leu) or selective
584 (SD/-Trp/-Leu/-His/-Ade) medium. Cells were diluted in three concentrations from left to

585 right. (B) *ZmLBD5*, *ZmLBD33* and *ZmLBD44* was individually cloned into pXYc104 and
 586 pXYn106 vectors, and fused with C-terminal (YC) or N-terminal (YN) of YFP. The
 587 indicated plastid combinations were transiently co-expressed in tobacco.
 588



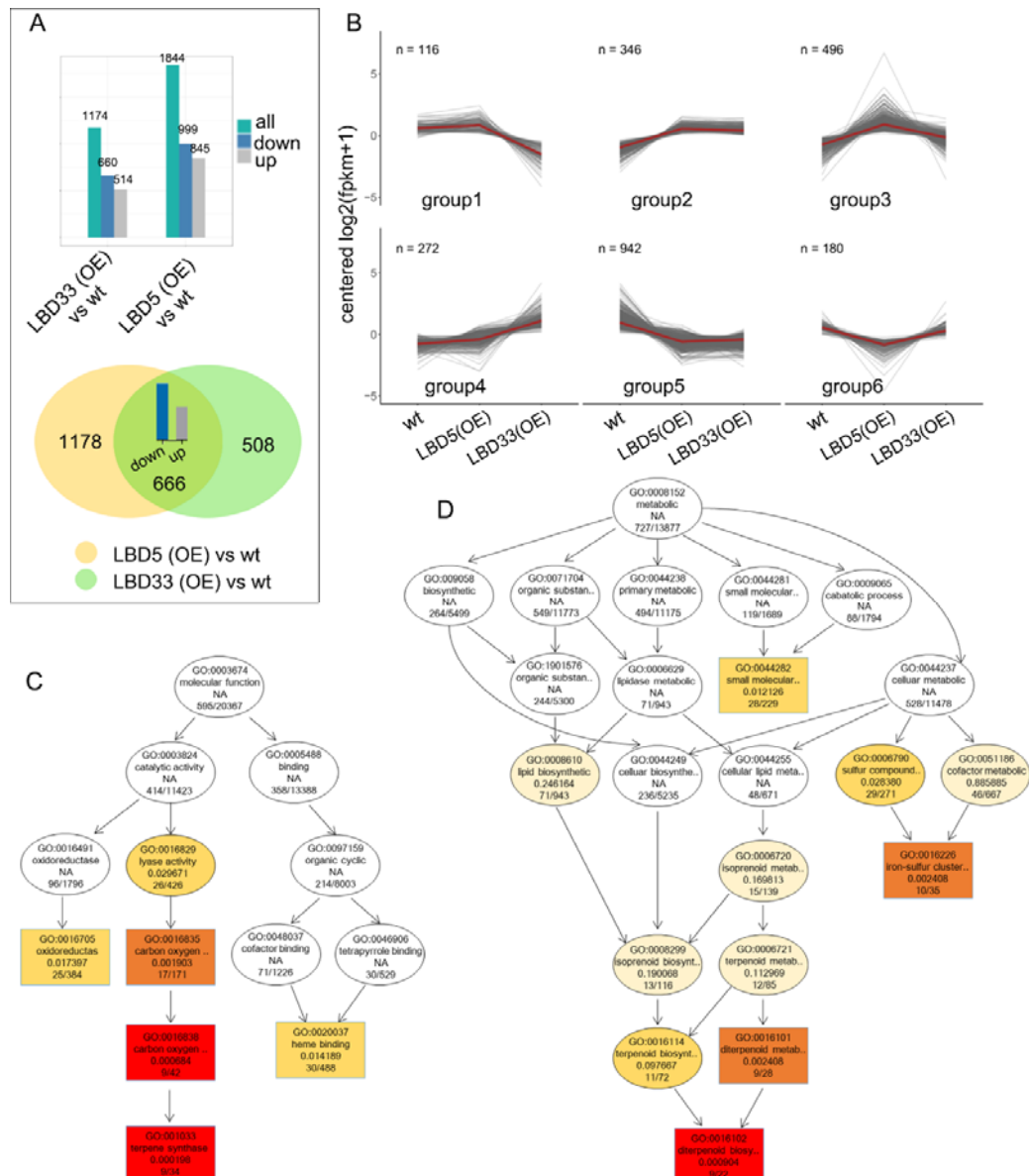
589
 590 **Figure 2. *ZmLBD5* or *ZmLBD33* over-expressed plants are drought sensitive.** (A)
 591 Wild type and individual transgenic lines were grown in separate pot exposed to well
 592 water or drought stress conditions. Quantitative description the phenotypes of root dry
 593 weight (B), shoot dry weight (C), ratio of dry weight between drought stress and well water
 594 conditions (D), shoot length (E) and leaf area (F). Ear phenotype (G), grain weight per ear
 595 (H), and hundred-grain weight (I) of transgenic plants and wild type in field upon well water
 596 and drought conditions. Asterisks on bar represent the difference compared with wild type
 597 is significant.
 598



599

600 **Figure 3. Overexpression of *ZmLBD5* or *ZmLBD33* promotes water loss.** (A) Water
 601 loss rate of detached leaf. (B) Soil moisture of each pot grown with wild type or different
 602 transgenic plants after the outage of water. (C) Stomata number of the third leaf on abaxial
 603 surface. (D) The ratio of open and closed stomata 15 minutes after detachment.
 604 Represented open and closed stomata were shown in the left panel. (E) Phenotype of
 605 seedlings before and after drought stress when different lines of transgenic plants and
 606 wild type were grown in the same pot. In panels (A), (B) and (D), if all three lines were
 607 significant different with the wild type asterisk was labeled.

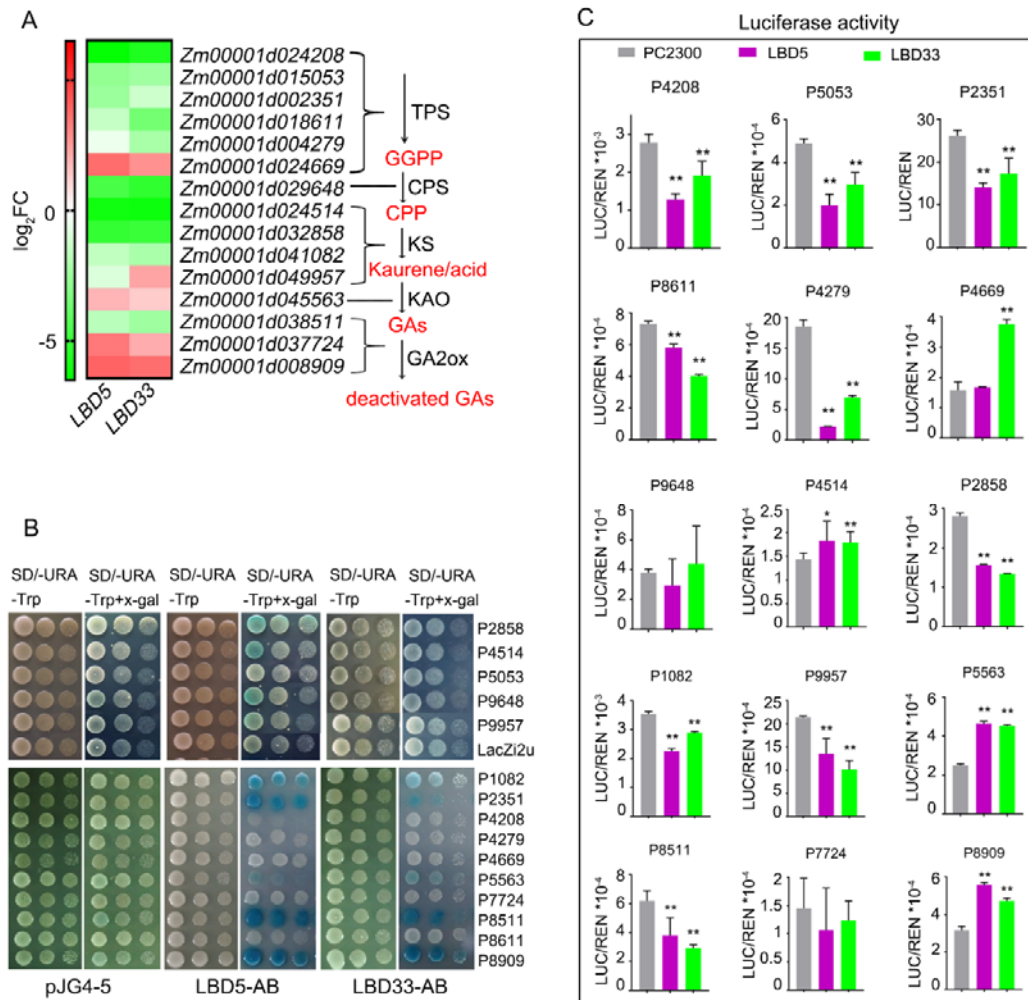
608



609

610 **Figure 4. RNA-seq indicates *ZmLBD5* and *ZmLBD33* function in terpenoid**
 611 **metabolic pathway.** (A) Different expressed gene (DEG) number in *LBD5* or *LBD33*
 612 overexpressed plants compared with the wild type. The fold change larger than 2 or
 613 smaller than 0.5 were determined as DEGs. (B) All of the DEGs were classified into 6
 614 groups by the centered and logarithmic transformed expression levels in wild type, *LBD5*
 615 (OE) and *LBD33* (OE). Directed Acyclic Graph of gene ontology enrichment analysis by
 616 using DEGs from *LBD5* overexpressed plants (C) and *LBD33* overexpressed plants (D).
 617 The four lines of information in each circle represent GO number, function annotation,
 618 P-value of GO enrichment significance test, and DEG number/background gene number,
 619 respectively. The darker the circle, the higher the enrichment.

620



621

622 **Figure 5. ZmLBD5 and ZmLBD33 directly regulate TPS-KS-GA2ox gene module.** (A)

623 15 DEGs in the most enriched GO terms in figure 4C and 4D were listed. The expression

624 fold change (FC) was converted to a logarithmic scale with base 2 and shown as different

625 color. TPS: terpene synthase; CPS: *ent*-copalyl diphosphate synthase; KS: *ent*-kaurene

626 synthase; KAO: *ent*-kaurenoic acid oxidase; GA2ox: GA 2-oxidase; GGPP:

627 geranylgeranyl diphosphate; CPP: *ent*-copalyl diphosphate. (B) Y1H testing whether

628 AB-segment of LBD5 and LBD33 bind to the promoters of five candidate genes. The yeast

629 cells harboring the indicated plastid combinations were grown on nonselective

630 (SD/-Ura/-Trp) or color development (SD/-Ura/-Trp/+x-gal) medium. The last four number

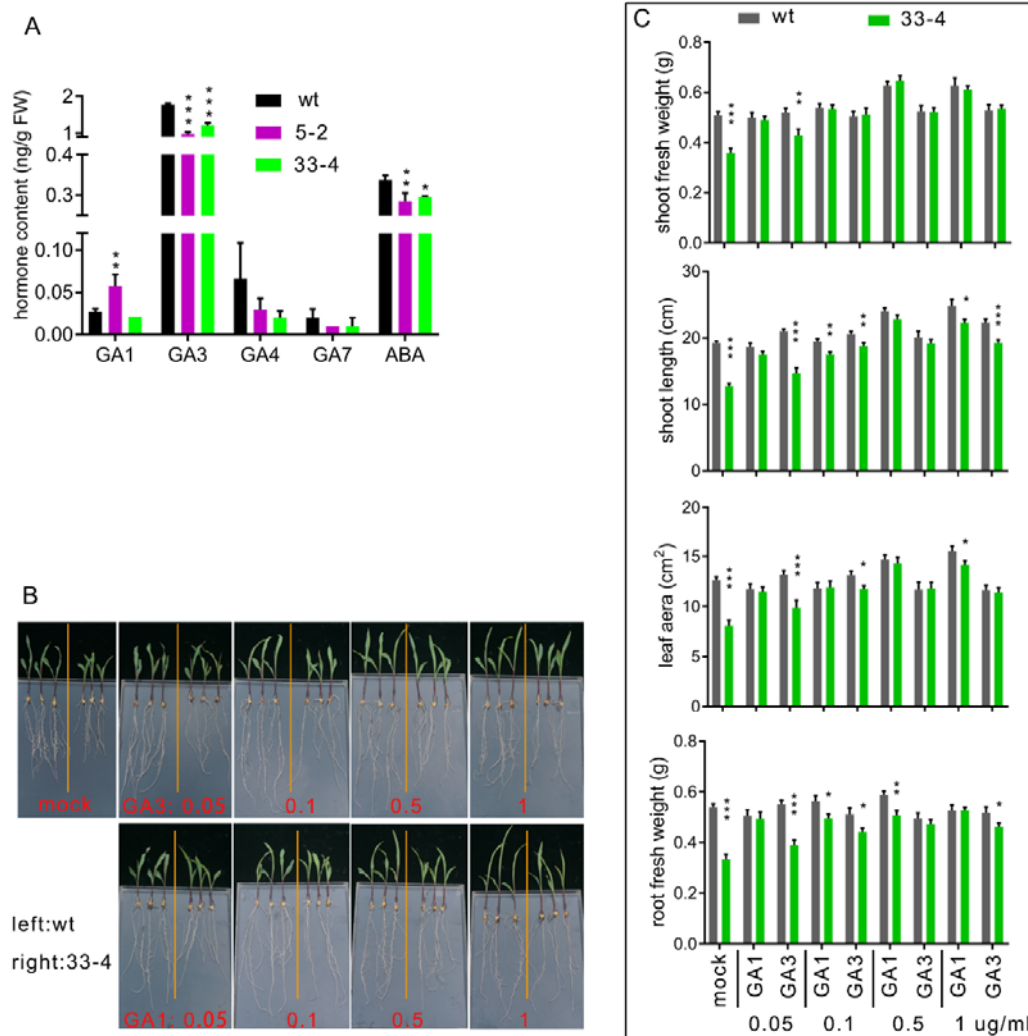
631 of the candidate gene name was used to represent corresponding gene. Cells were

632 diluted in three concentrations from left to right. (C) dual-luciferase reporter system was

633 used to investigate the regulation of LBD5/LBD33 on candidate genes. Asterisks on bar

634 represent the difference compared with wild type is significant.

635



636

637 **Figure 6. Exogenous GA₁ and GA₃ rescue the dwarf phenotype of *ZmLBD33***
 638 **overexpressed plants.** (A) Endogenous content of GAs and ABA of 12-days-old
 639 seedlings. (B) Phenotype and (C) quantitative description of shoot length, leaf area, shoot
 640 fresh weight and root fresh weight. Asterisks on bar represent the difference compared
 641 with wild type is significant.

642

643

644

645

646

647

648

649

650

651

652

653 **Supplemental materials**

A

```

LBD5 MRMSCNGCRVLRKGCSDACTI RPCLQW KSPEAQANATVFLAKFYGRAGLLNLLAAPPADHLRPAAFRSLLYEACGRI VN 80
LBD33 MRMSCNGCRVLRKGCSDACTI RPCLQW DSPEAQANATVFLAKFYGRAGLLNLLAAPPDAAARPAVFRSLLYEACGRI VN 80

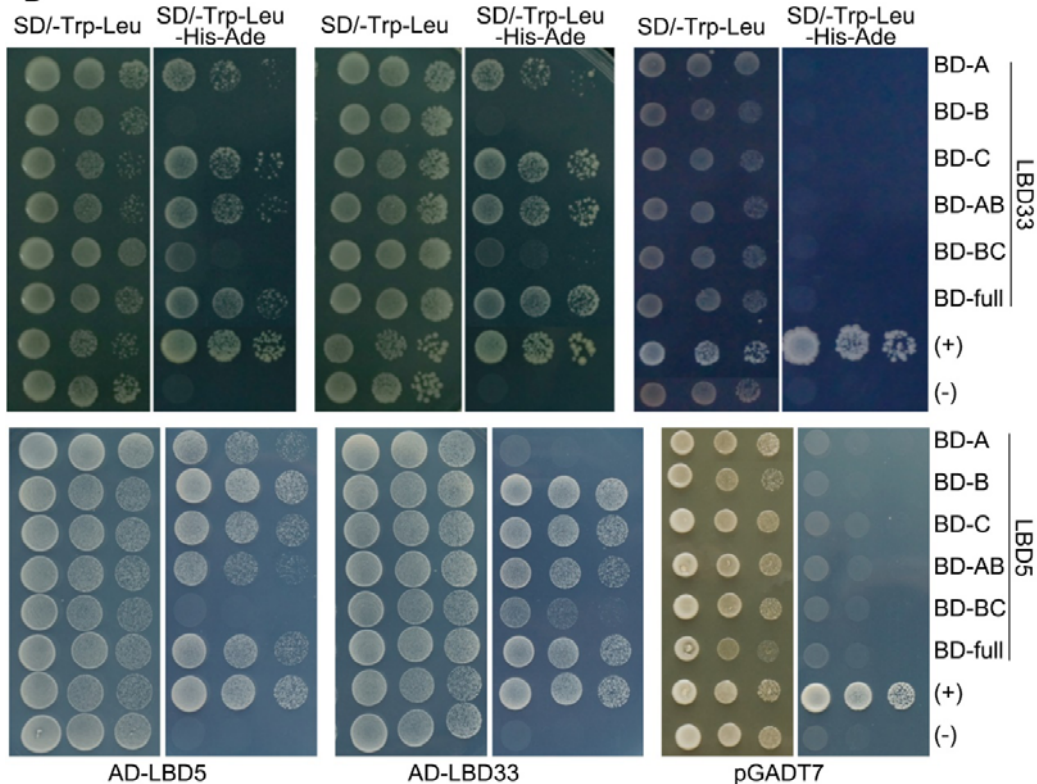
LBD5 PVYGSVGLLWSGQWQACQAAVEAVLKGDPV VQVQV-- DAASDASPPLGPRR- - - - - HDI RHVARDP- - AAAPDVL- - L 147
LBD33 PVYGSVGLLWSRRWQSCVDAVEAVLKGDPVVQVDAGSEAAAAAPALLGASRPAAPPAAYDI RHVARDPDAVAADLLRVA 160

LBD5 RSSSR- - - KRAASSTSSKHN- - - QPGSSKRA SLGKNRQRAEQE- - - - - PVPMVVE- - HGEESAGSHDHDHQQHRL 211
LBD33 RGGGRRRFKRA GSSNACKAKPLK GKASSNERASPSPTQRQHQQETE EEELEPVP MVVELEHGEESAGSHDHHH- - HLQP 238

LBD5 QGSEEDTDVEAASHAHSHV SQAEP EPEPETEPQSHAPPA CSQQANQEHQDDEDEELALEL TLGLEPLVRQRQRPKSSRS 291
LBD33 QGSEEDTDVEAAS- - - HYSQAEAE P- - - - - PVYSSQALVADQ- - EGEEVRL E L TLGFEPVVRQQPR- - - - L S 297

LBD5 DCDHSGLSAASSLMCLRLQLPA 313
LBD33 CCDSSGLSAASSLI GLRLQLPAA 320
    
```

B



654

655

656

657

658

659

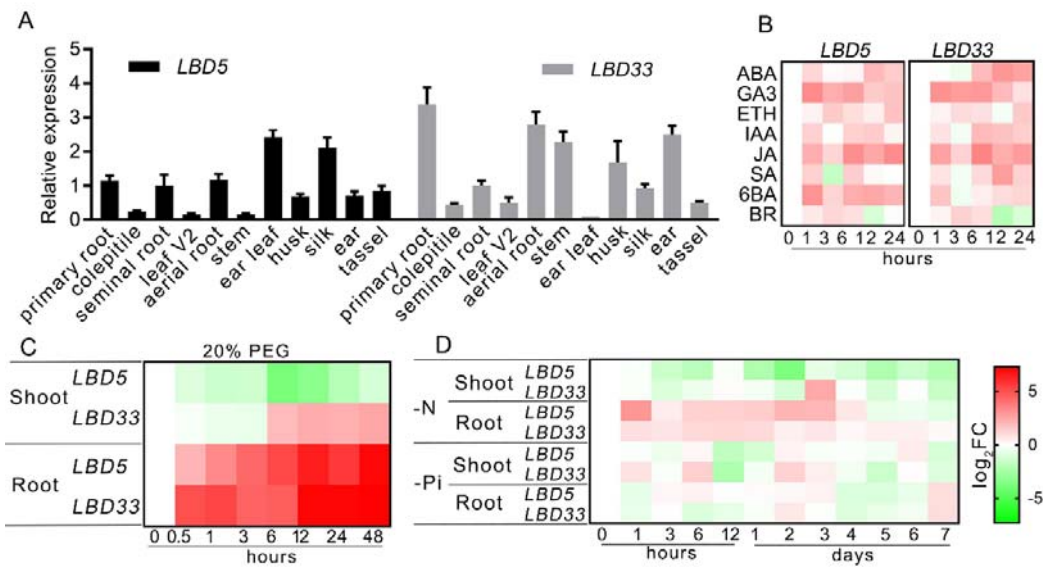
660

661

662

663

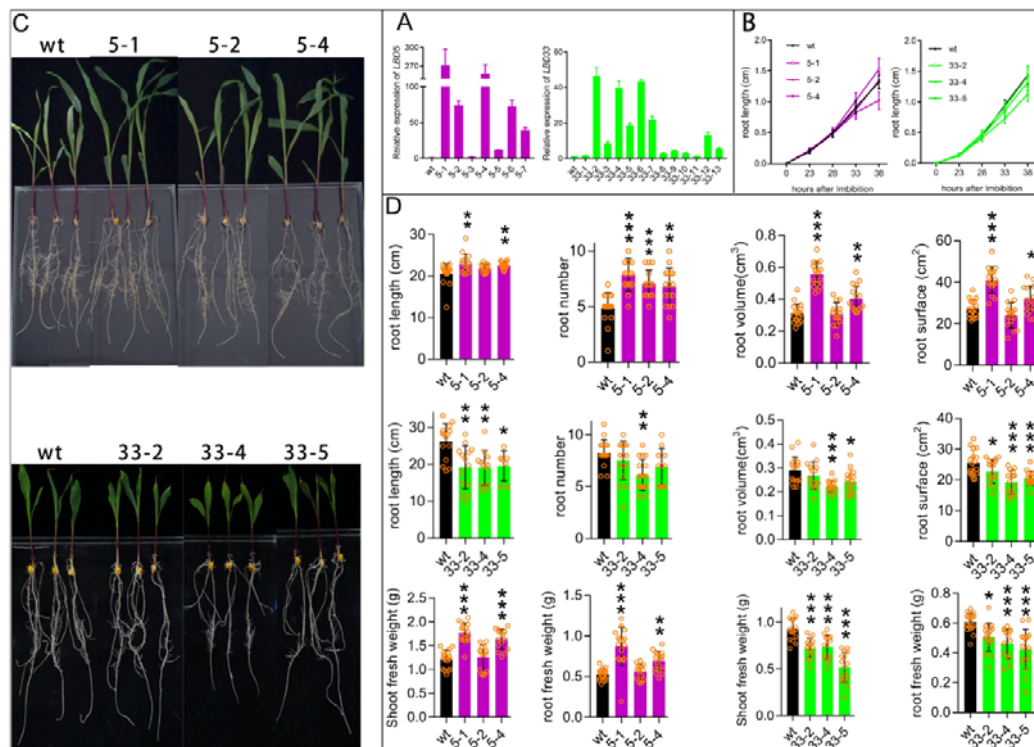
Figure S1. Investigation of the hetero- and homo- protein-protein interaction of ZmLBD5 and ZmLBD33. (A) Three segments of ZmLBD5 and ZmLBD33 were divided from red arrows indicated two sites. (B) Different segments of ZmLBD5 and ZmLBD33 were cloned into pGBK-T7 and fused with BD. Full codon region of ZmLBD5 and ZmLBD33 were cloned into pGAD-T7 and fused with AD. The yeast cells harboring the indicated plasmid combinations were grown on nonselective (SD/-Trp/-Leu) or selective (SD/-Trp/-Leu/-His/-Ade) medium. Cells were diluted in three concentrations from left to right.



664

665 **Figure S2. Expression of *ZmLBD5* and *ZmLBD33* upon different tissues and**
 666 **different stimuli.** (A) Expression of *ZmLBD5* and *ZmLBD33* in different tissues, (B) upon
 667 different phytohormones, (C) upon PEG caused osmotic stress, (D) upon nitrogen or
 668 phosphorus deficiency. Fold change of expression relative to 0 point of treatment is
 669 converted to a logarithmic scale with base 2 and shown as different color in (B), (C), and
 670 (D).
 671

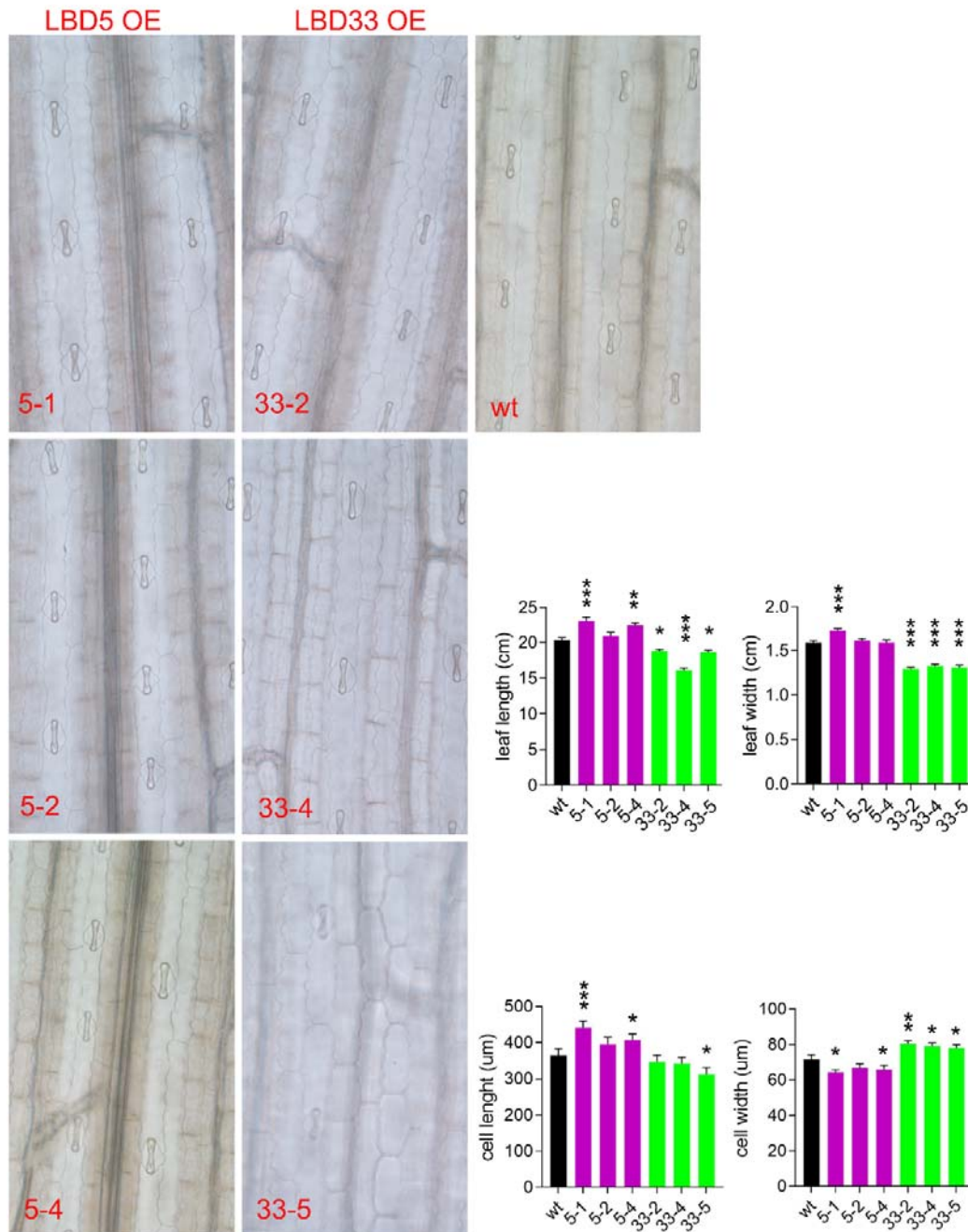
671



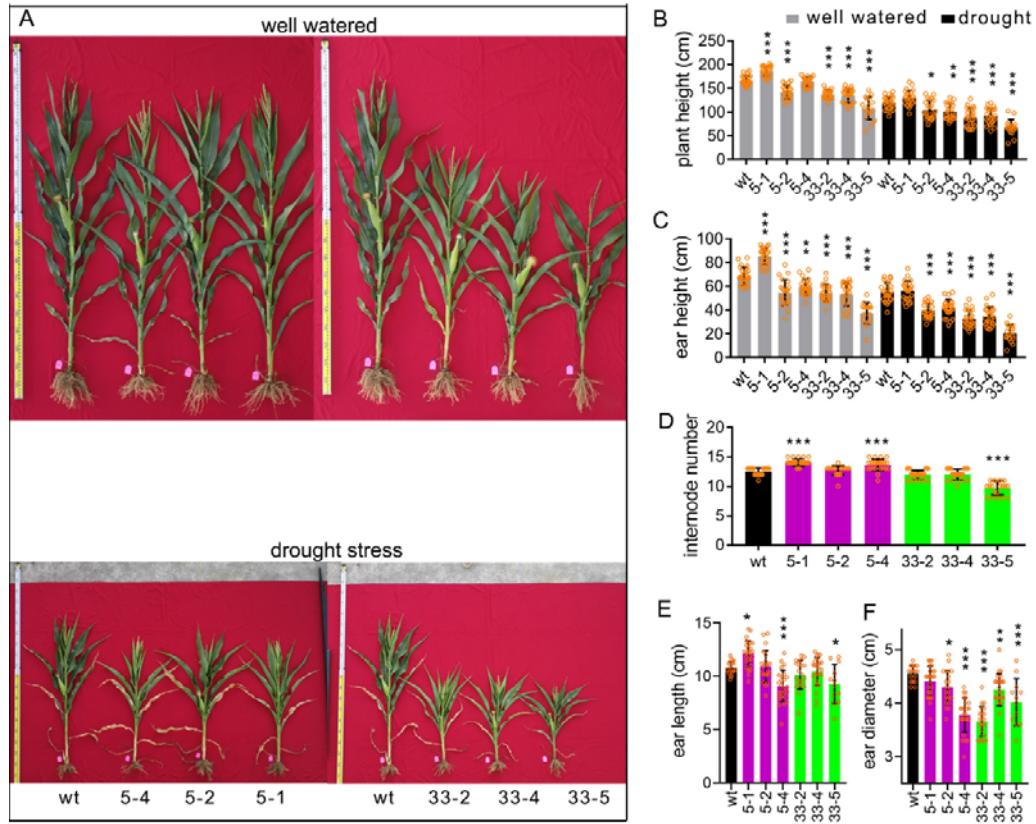
672

673 **Figure S3. Phenotypic investigation of representative transgenic lines upon**

674 **hydroponic conditions.** (A) Relative expression of *LBD5* and *LBD33* in different
 675 transgenic lines. (B) The primary root length at different time after imbibition. (C)
 676 Phenotype and (D) quantitative description of primary root length, root number, root
 677 volume, root surface, shoot fresh weight and root fresh weight. Asterisks on bar represent
 678 the difference compared with wild type is significant.
 679



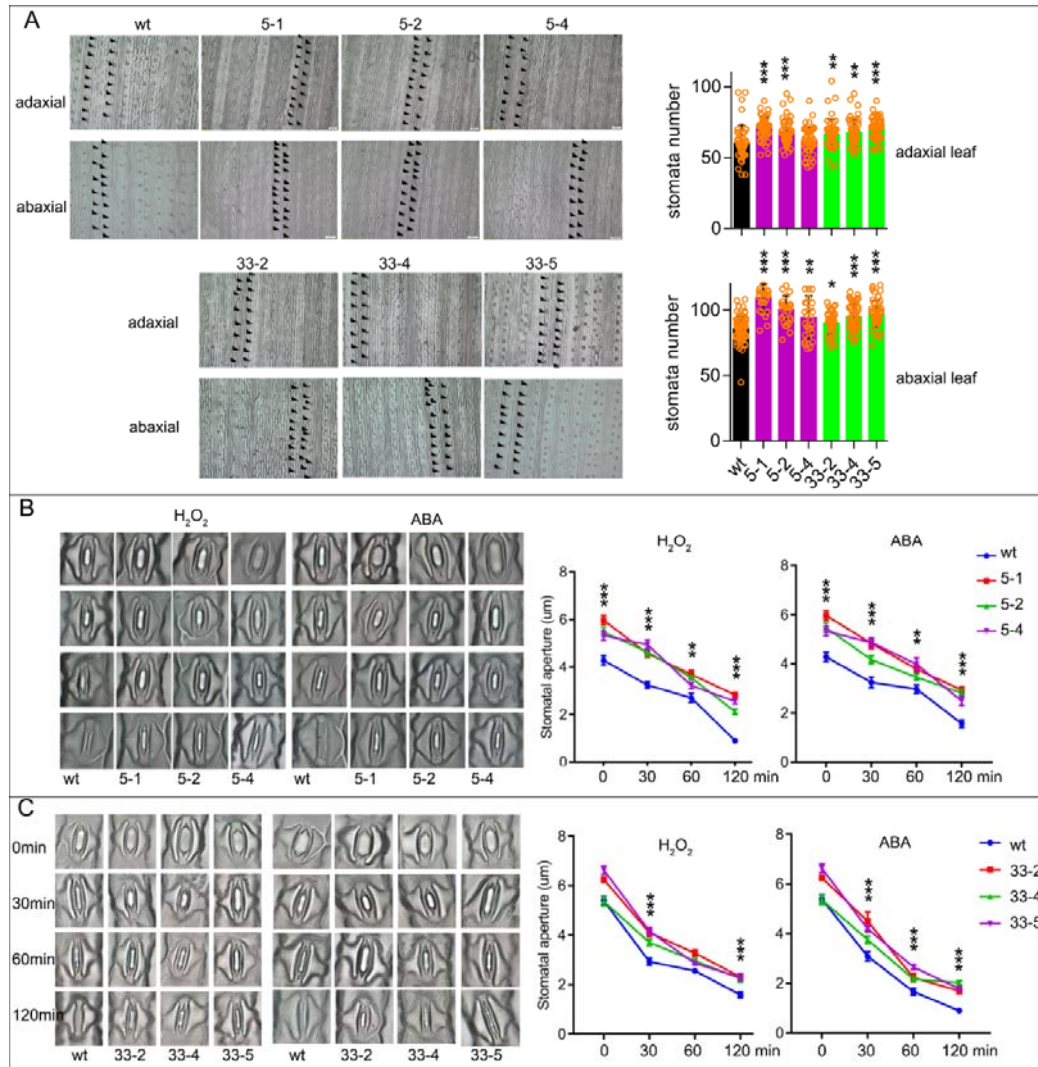
680
 681 **Figure S4. Microscale phenotype of third leaf on adaxial surface, cell length, cell**
 682 **width, leaf length and leaf width.** Asterisks on bar represent the difference compared
 683 with wild type is significant.



684

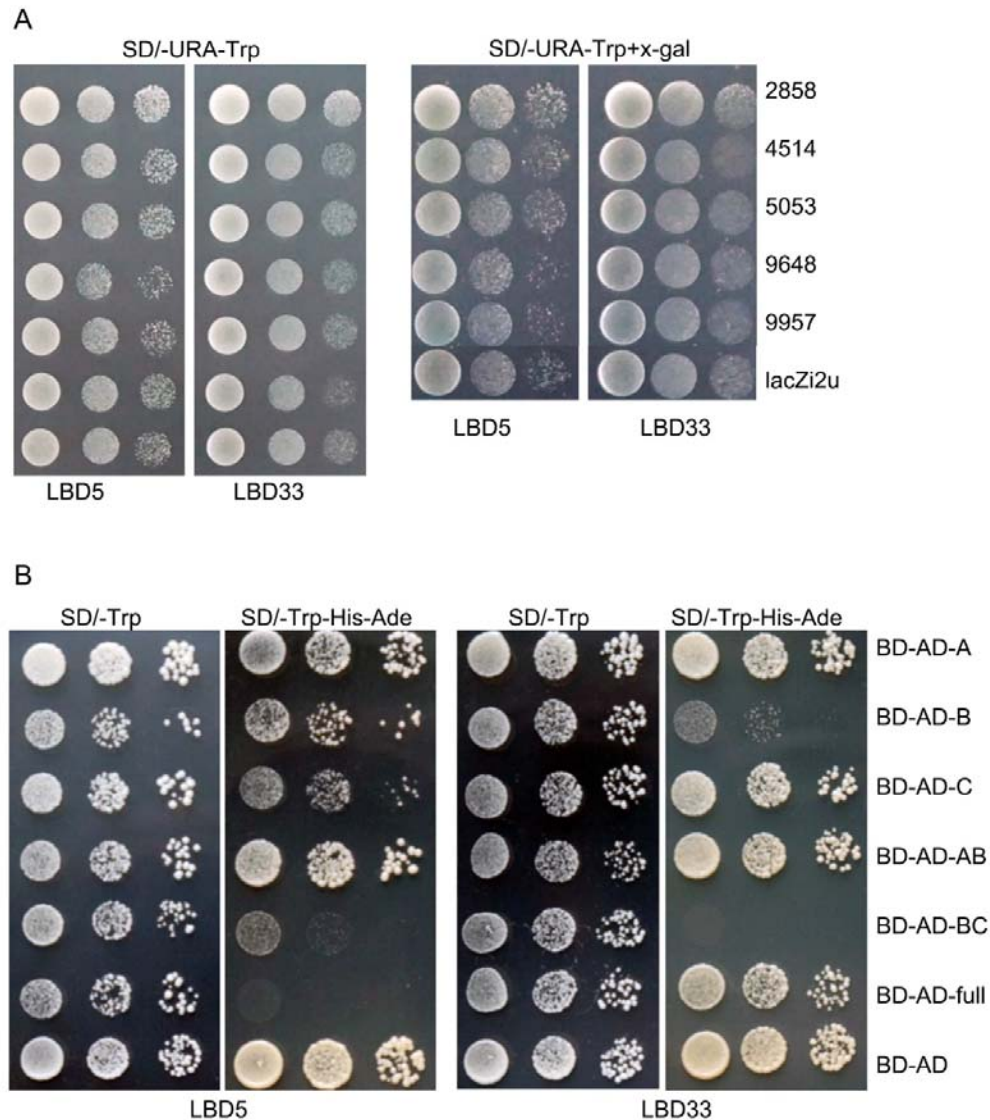
685 **Figure S5. Phenotype of plants after tasseling.** (A) Representative plants under well
686 water condition. Plant height (B), Ear height (C), and internode number (D) of transgenic
687 plants and wild type in field upon well water and drought conditions. Asterisks on bar
688 represent the difference compared with wild type is significant.

689



690

691 **Figure S6. Stomata number and stomatal aperture upon ABA or H₂O₂ treatment. (A)**
 692 Stomata number of the third leaf on abaxial surface and adaxial surface. Stomatal
 693 aperture of *LBD5* (B) and *LBD33* (C) overexpressed plants after ABA or H₂O₂ treatment.
 694 Asterisks on bar represent the difference compared with wild type is significant. In B and C,
 695 if all three lines were significant different with the wild type asterisk was labeled.
 696



697

698 **Figure S7. Yeast one-hybrid and potential transcriptional inhibition activity of LBD5**

699 **and LBD33.** (A) The yeast cells harboring the indicated plastid combinations were grown

700 on nonselective (SD/-Ura/-Trp) or color development (SD/-Ura/-Trp/+x-gal) medium. The

701 last four number of the candidate gene name was used to represent corresponding gene.

702 (B) Different segments of LBD5 and LBD33 were fused with Gal4-AD and cloned into

703 pGBK-T7 to fuse with Gal4-BD. The yeast cells harboring indicated construct were grown

704 on nonselective (SD/-Trp) or selective (SD/-Trp/-His/-Ade) medium. Cells were diluted in

705 three concentrations from left to right.

706

707

708 **Table S1. internode length of plants after tasseling in field.**

709 **Table S2. DEGs in LBD5- and LBD33- overexpressing plant.**

710 **Table S3. Enriched GO terms and gene list in GGPP-CPP-kaurene/acid-GA**

- 711 **metabolism and P450 members.**
712 **Table S4. Plasmid constructs and primers used in this study.**
713 **Table S5. primers for real-time qPCR.**

Parsed Citations

- Albinsky D, Kusano M, Higuchi M, Hayashi N, Kobayashi M, Fukushima A, Mori M, Ichikawa T, Matsui K, Kuroda H, Horii Y, Tsumoto Y, Sakakibara H, Hirochika H, Matsui M, Saito K (2010) Metabolomic screening applied to rice FOX Arabidopsis lines leads to the identification of a gene-changing nitrogen metabolism. Mol Plant 3: 125-142**
Google Scholar: [Author Only](#) [Title Only](#) [Author and Title](#)
- Bao S, Hua C, Shen L, Yu H (2020) New insights into gibberellin signaling in regulating flowering in Arabidopsis. J Integr Plant Biol 62: 118-131**
Google Scholar: [Author Only](#) [Title Only](#) [Author and Title](#)
- Bortiri E, Chuck G, Vollbrecht E, Rocheford T, Martienssen R, Hake S (2006) ramosa2 encodes a LATERAL ORGAN BOUNDARY domain protein that determines the fate of stem cells in branch meristems of maize. Plant Cell 18: 574-585**
Google Scholar: [Author Only](#) [Title Only](#) [Author and Title](#)
- Chen Y, Hou M, Liu L, Wu S, Shen Y, Ishiyama K, Kobayashi M, McCarty DR, Tan BC (2014) The maize DWARF1 encodes a gibberellin 3-oxidase and is dual localized to the nucleus and cytosol. Plant Physiol 166: 2028-2039**
Google Scholar: [Author Only](#) [Title Only](#) [Author and Title](#)
- Colebrook EH, Thomas SG, Phillips AL, Hedden P (2014) The role of gibberellin signalling in plant responses to abiotic stress. J Exp Biol 217: 67-75**
Google Scholar: [Author Only](#) [Title Only](#) [Author and Title](#)
- Du H, Chang Y, Huang F, Xiong L (2015) GID1 modulates stomatal response and submergence tolerance involving abscisic acid and gibberellic acid signaling in rice. J Integr Plant Biol 57: 954-968**
Google Scholar: [Author Only](#) [Title Only](#) [Author and Title](#)
- Evans MM (2007) The indeterminate gametophyte1 gene of maize encodes a LOB domain protein required for embryo Sac and leaf development. Plant Cell 19: 46-62**
Google Scholar: [Author Only](#) [Title Only](#) [Author and Title](#)
- Feng XJ, Li JR, Qi SL, Lin QF, Jin JB, Hua XJ (2016) Light affects salt stress-induced transcriptional memory of P5CS1 in Arabidopsis. Proc Natl Acad Sci U S A 113: E8335-E8343**
Google Scholar: [Author Only](#) [Title Only](#) [Author and Title](#)
- Fu J, Ren F, Lu X, Mao H, Xu M, Degenhardt J, Peters RJ, Wang Q (2016) A Tandem Array of ent-Kaurene Synthases in Maize with Roles in Gibberellin and More Specialized Metabolism. Plant Physiol 170: 742-751**
Google Scholar: [Author Only](#) [Title Only](#) [Author and Title](#)
- He J, Xin P, Ma X, Chu J, Wang G (2020) Gibberellin Metabolism in Flowering Plants: An Update and Perspectives. Front Plant Sci 11: 532**
Google Scholar: [Author Only](#) [Title Only](#) [Author and Title](#)
- Hedden P (2003) The genes of the Green Revolution. Trends Genet 19: 5-9**
Google Scholar: [Author Only](#) [Title Only](#) [Author and Title](#)
- Hedden P, Phillips AL (2000) Gibberellin metabolism: new insights revealed by the genes. Trends in Plant Science 5: 523-530**
Google Scholar: [Author Only](#) [Title Only](#) [Author and Title](#)
- Hedden P, Proebsting WM (1999) Genetic Analysis of Gibberellin Biosynthesis. Plant Physiol 119: 365-370**
Google Scholar: [Author Only](#) [Title Only](#) [Author and Title](#)
- Hedden P, Sponsel V (2015) A Century of Gibberellin Research. J Plant Growth Regul 34: 740-760**
Google Scholar: [Author Only](#) [Title Only](#) [Author and Title](#)
- Iwakawa H, Iwasaki M, Kojima S, Ueno Y, Soma T, Tanaka H, Semiarti E, Machida Y, Machida C (2007) Expression of the ASYMMETRIC LEAVES2 gene in the adaxial domain of Arabidopsis leaves represses cell proliferation in this domain and is critical for the development of properly expanded leaves. Plant J 51: 173-184**
Google Scholar: [Author Only](#) [Title Only](#) [Author and Title](#)
- Majer C, Hochholdinger F (2011) Defining the boundaries: structure and function of LOB domain proteins. Trends Plant Sci 16: 47-52**
Google Scholar: [Author Only](#) [Title Only](#) [Author and Title](#)
- Majer C, Xu C, Berendzen KW, Hochholdinger F (2012) Molecular interactions of ROOTLESS CONCERNING CROWN AND SEMINAL ROOTS, a LOB domain protein regulating shoot-borne root initiation in maize (Zea mays L.). Philos Trans R Soc Lond B Biol Sci 367: 1542-1551**
Google Scholar: [Author Only](#) [Title Only](#) [Author and Title](#)
- Mehrotra R, Bhalothia P, Bansal P, Basantani MK, Bharti V, Mehrotra S (2014) Abscisic acid and abiotic stress tolerance - different tiers of regulation. J Plant Physiol 171: 486-496**
Google Scholar: [Author Only](#) [Title Only](#) [Author and Title](#)
- Nagai K, Mori Y, Ishikawa S, Furuta T, Gamuyao R, Niimi Y, Hobo T, Fukuda M, Kojima M, Takebayashi Y, Fukushima A, Himuro Y,**

Kobayashi M, Ackley W, Hisano H, Sato K, Yoshida A, Wu J, Sakakibara H, Sato Y, Tsuji H, Akagi T, Ashikari M (2020) Antagonistic regulation of the gibberellic acid response during stem growth in rice. *Nature* 584: 109-114

Google Scholar: [Author Only](#) [Title Only](#) [Author and Title](#)

Rubin G, Tohge T, Matsuda F, Saito K, Scheible WR (2009) Members of the LBD family of transcription factors repress anthocyanin synthesis and affect additional nitrogen responses in Arabidopsis. *Plant Cell* 21: 3567-3584

Google Scholar: [Author Only](#) [Title Only](#) [Author and Title](#)

Scheible WR, Morcuende R, Czechowski T, Fritz C, Osuna D, Palacios-Rojas N, Schindelasch D, Thimm O, Udvardi MK, Stitt M (2004) Genome-wide reprogramming of primary and secondary metabolism, protein synthesis, cellular growth processes, and the regulatory infrastructure of Arabidopsis in response to nitrogen. *Plant Physiol* 136: 2483-2499

Google Scholar: [Author Only](#) [Title Only](#) [Author and Title](#)

Semiarti E, Ueno Y, Tsukaya H, Iwakawa H, Machida C, Machida Y (2001) The ASYMMETRIC LEAVES2 gene of Arabidopsis thaliana regulates formation of a symmetric lamina, establishment of venation and repression of meristem-related homeobox genes in leaves. *Development* 128: 1771-1783

Google Scholar: [Author Only](#) [Title Only](#) [Author and Title](#)

Shuai B, Reynaga-Pena CG, Springer PS (2002) The lateral organ boundaries gene defines a novel, plant-specific gene family. *Plant Physiol* 129: 747-761

Google Scholar: [Author Only](#) [Title Only](#) [Author and Title](#)

Spray CR, Kobayashi M, Suzuki Y, Phinney BO, Gaskin P, MacMillan J (1996) The dwarf-1 (d1) Mutant of Zea mays blocks three steps in the gibberellin-biosynthetic pathway. *Proc Natl Acad Sci U S A* 93: 10515-10518

Google Scholar: [Author Only](#) [Title Only](#) [Author and Title](#)

Taramino G, Sauer M, Stauffer JL, Jr., Multani D, Niu X, Sakai H, Hochholdinger F (2007) The maize (*Zea mays* L.) RTCS gene encodes a LOB domain protein that is a key regulator of embryonic seminal and post-embryonic shoot-borne root initiation. *Plant J* 50: 649-659

Google Scholar: [Author Only](#) [Title Only](#) [Author and Title](#)

Teng F, Zhai L, Liu R, Bai W, Wang L, Huo D, Tao Y, Zheng Y, Zhang Z (2013) ZmGA3ox2, a candidate gene for a major QTL, qPH3.1, for plant height in maize. *Plant J* 73: 405-416

Google Scholar: [Author Only](#) [Title Only](#) [Author and Title](#)

White CN, Proebsting WM, Hedden P, Rivin CJ (2000) Gibberellins and Seed Development in Maize. I. Evidence That Gibberellin-Absciscic Acid Balance Governs Germination versus Maturation Pathways. *Plant Physiol* 122: 1081-1088

Google Scholar: [Author Only](#) [Title Only](#) [Author and Title](#)

Xiong L, Zhu JK (2003) Regulation of abscisic acid biosynthesis. *Plant Physiol* 133: 29-36

Google Scholar: [Author Only](#) [Title Only](#) [Author and Title](#)

Xu C, Luo F, Hochholdinger F (2016) LOB Domain Proteins: Beyond Lateral Organ Boundaries. *Trends Plant Sci* 21: 159-167

Google Scholar: [Author Only](#) [Title Only](#) [Author and Title](#)

Xu C, Tai H, Saleem M, Ludwig Y, Majer C, Berendzen KW, Nagel KA, Wojciechowski T, Meeley RB, Taramino G, Hochholdinger F (2015) Cooperative action of the paralogous maize lateral organ boundaries (LOB) domain proteins RTCS and RTCL in shoot-borne root formation. *New Phytol* 207: 1123-1133

Google Scholar: [Author Only](#) [Title Only](#) [Author and Title](#)

Yu Q, Hu S, Du J, Yang Y, Sun X (2020) Genome-wide identification and characterization of the lateral organ boundaries domain gene family in Brassica rapa var. rapa. *Plant Divers* 42: 52-60

Google Scholar: [Author Only](#) [Title Only](#) [Author and Title](#)

Zhang Y-m, Zhang S-z, Zheng C-c (2014) Genomewide analysis of LATERAL ORGAN BOUNDARIES Domain gene family in Zea mays. *J Genet* 93: 79-91

Google Scholar: [Author Only](#) [Title Only](#) [Author and Title](#)

Zimmermann R, Sakai H, Hochholdinger F (2010) The Gibberellic Acid Stimulated-Like gene family in maize and its role in lateral root development. *Plant Physiol* 152: 356-365

Google Scholar: [Author Only](#) [Title Only](#) [Author and Title](#)